Roles of nonlocal conductivity on spin Hall angle measurement

Kai Chen and Shufeng Zhang

Phys. Rev. B **96**, 134401 — Published 2 October 2017

DOI: 10.1103/PhysRevB.96.134401

Roles of non-local conductivity on spin Hall angle measurement

Kai Chen and Shufeng Zhang

Department of Physics, University of Arizona, Tucson AZ 85721

Abstract

Spin Hall angle characterizes the rate of spin-charge current conversion and it has become one of the most important material parameters for spintronics physics and device application. A long standing controversy is that the spin Hall angles for a given material measured by the spin pumping and by the spin Hall torque experiments are inconsistent and they could differ as large as an order of magnitude. By using the linear response spin transport theory, we explicitly formulate the relation between the spin Hall angle and measured variables in different experiments. We find that the non-local conductivity inherited in the layered structure plays a key role to resolve conflicting values of the spin Hall angle. We provide a generalized scheme for extracting spin transport coefficients from experimental data.

I. INTRODUCTION

Spin Hall (SH) and inverse spin Hall (ISH) effects provide an efficient way to convert charge-to-spin and spin-to-charge currents[1,2]. Spin Hall angle θ_H quantitatively characterizes the conversion rate: SH yields a spin current $j_s = \theta_H(\hbar/2e)j_e$ from the applied electric current density j_e, and ISH generates an electric current $j_e = \theta_H(2e/\hbar)j_s$ from the injected spin current j_s. Since there are no "spin current meters" to directly measure the spin current, one obtains the spin Hall angle by indirectly measuring the spin current. The first measurement was achieved via optical Keer effect where spin accumulation at the edge of the sample is detected[3], but no quantitative values of θ_H were obtained. The electric measurement based on spin transfer torques (STT)[4–12] and ISH voltage[13–19] from spin pumping (SP) or spin Seebeck (SS) are currently used to quantitatively determine the spin Hall angle. Both methods utilize a bilayer structure made of a ferromagnetic (FM) layer and a non-magnetic (NM) layer. Typically, the non-magnetic layer is a heavy metal of which the spin Hall angle is measured. In STT, an applied in-plane charge current in the heavy metal converts to the spin current flowing perpendicularly to the layers, and subsequent spin current absorption creates a spin torque on the ferromagnetic layer. Thus, the spin Hall angles are determined through the measurement of the current-induced spin torque. In ISH voltage measurement, a spin current is generated by either the spin pumping from the precessing ferromagnetic layer or by a thermal gradient in the magnetic layer. The spin current injected to the heavy metal by SP or SS subsequently converts to an electric charge current in the plane of the layer, yielding a measurable voltage. While both methods have been widely studied for different materials, the experimentally deduced values of θ_H have consistently differed by a large margin, from several tens to a few hundred percentage, see Figure 1 for the experimental data from literature. Up until now, there is no consensus agreement on the proper value of the spin Hall angle for well-studied materials such as Pt, W, and Ta, due to apparently conflicting results among experimental groups. Without firmly established experimental values, it would be difficult to compare the results with first-principle calculations[20,21].

Similar to the uncertainty of the spin Hall angle, the values of the spin diffusion length are widely spread as well. Since spin diffusion and spin Hall effect come from the same physical origin in spin-orbit coupling, a large spin Hall angle would be likely associated with a smaller spin diffusion length. Indeed, the correlation between these two parameters

have been approximately obtained by using the same fitting procedure[22]. The spin diffusion length is also shown to correlate with resistivity[23]. Thus, the quantitative determination of the spin Hall angle would be critical to reveal connections among these spin transport coefficients. In this paper, we theoretically formulate the relation between the spin Hall angle and the measured variables of the above experimental measurements. As the layer thickness of the experimental bilayers are often of the order of the electron mean free path, we find the non-local conductivity in these experiments plays crucial roles, and thereby significant corrections to the previously claimed spin Hall angles in different experiments are required.

The paper is organized as follows. In Sec. II, we first demonstrate that the measured spin Hall angles via both ISH and STT deviate from the true value due to the effects of nonlocal conductivity. Then, we outlined the method how we calculate the conductivity in thin films. In Sec. III, we apply our methods to heavy metal bilayers. The influence of nonlocal conductivity is evaluated numerically at various parameters. Some discussion about the conductivity contribution from interface states is included in the Appendix.

II. THEORETICAL DERIVATION

A. Spin Hall Angle Measurement

We start with the ISH method (spin pumping or spin Seebeck) in which a spin current j_s is injected from the ferromagnetic layer to the heavy metal. By considering the process of the spin diffusion and spin current backflow, the spin current in the heavy metal decays as $j_s(z) = j_s(0)\sinh\left[(d_N - z)/\lambda_s\right]/\sinh\left(d_N/\lambda_s\right)$ where $j_s(0)$ is the spin current density at the interface and λ_s is the spin diffusion length and d_N is the thickness of the NM layer[24]. The spin current yields an in-plane electric field $E_{sh}(z) = \theta_H \rho_N j_s(z)$ where ρ_N is the resistivity of the *bulk* heavy metal; for simplicity we take $\hbar = e = 1$ so that the unit of spin current is same as that of the charge current. The use of the bulk value of the resistivity indicates that θ_H is defined as to the spin Hall angle of the bulk. This electric field serves as an electric motive force of the inverse spin Hall effect that generates an electric current in the plane of the layers (CIP). In the open boundary condition, a charge accumulation at the sample boundary, or equivalently, the *measured* electric field E_m must be established to oppose the

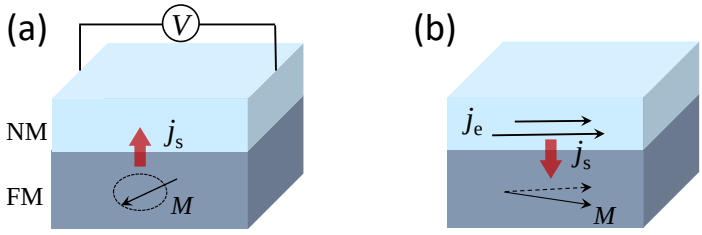

ISH voltage Spin transfer torque

Heavy Metal	θ_H from ISH	θ_H from STT
Pt	0.012[13], 0.013[14], 0.013[15], 0.027[16], 0.03[17], 0.08[18], 0.1[19]	0.04[9], 0.08[4], 0.19[8]
Ta	-0.02[17], -0.07[19]	-0.15[10], -0.2[7]
W	-0.14[19]	-0.2[11], -0.3[5], -0.5[12]

FIG. 1: (Color Online) Spin Hall angle of a heavy metal is obtained by two experimental measurements. (a) A precessing magnetic layer pumps the spin current into the heavy metal. An electric field (or a charge voltage) from the ISH effect is measured. (b) An applied in-plane electric current accompanies a spin current flowing perpendicular to the layer due to SH effect. The spin current exerts a torque on the ferromagnetic layer which is being measured. The table of the spin Hall angles shows a wide range of values for these two classes of measurement. The spin diffusion length varies with a similar wide spread (not shown)[22].

spin Hall induced electric motive force E_{sh} such that the total electric current is zero, i.e.,

$$\int_{-d_F}^{d_N} j_e(z)dz = \int_{-d_F}^{d_N} dz \int_{-d_F}^{d_N} dz' \sigma_{||}(z,z') \left[E_m + E_{sh}(z')\right] = 0 \tag{1}$$

where $\sigma_{||}(z,z')$ is the in-plane two-point conductivity tensor of the bilayer. Solving for the measured electric field from the above equation, we have

$$E_m = G_t^{-1} \rho_N \theta_{\rm sh} \int_0^{d_N} dz \sigma_{||}(z) j_s(z) \tag{2}$$

where $\sigma_{||}(z) = \int dz' \sigma_{||}(z,z')$ is the position-dependent conductivity, $G_t = \int \sigma_{||}(z)dz$ is the total conductance, and we assume the ISH current only exists in the heavy metal. While the total conductance of the bilayer G_t can be experimentally measured and the spin current

$j_s(z)$ has been indirectly measured via the enhanced damping parameter[24], the position-dependent conductivity $\sigma_{||}(z)$ is needed in order to determine θ_H from the measured electric field E_m.

At present, the experimental data were fitted by the formula which is equivalent to taking the conductivity by its bulk value, $\sigma_{||}(z) = \rho_N^{-1}$ in Eq. (2), i.e., the spin Hall angle was determined by $\theta_H^{\rm ISH} = E_m G_t / (d_N \bar{j}_s)$, where $\bar{j}_s = \lambda_s d_N^{-1} j_s(0) \tanh\left(\frac{t_N}{2\lambda_s}\right)$ is the average current density in the heavy metal. Thus, the ratio of the *true* spin Hall angle θ_H from Eq. (2) and $\theta_H^{\rm ISH}$ of the value previously determined from ISH experiment is

$$R_{\rm ISH} \equiv \frac{\theta_H}{\theta_H^{\rm ISH}} = \frac{\int_0^{d_N} \sinh[(d_N - z)/\lambda_s] dz}{\rho_N \int_0^{d_N} \sigma_{||}(z) \sinh[(d_N - x)/\lambda_s] dz} \tag{3}$$

Clearly, $\sigma_{||}(z)$ from the two-point conductivity tensor in the bilayer includes the scattering from the interfaces and it could be much smaller than that of the conductivity of the bulk materials ρ_N^{-1} when the thickness of the layer is comparable or smaller than the mean free path. Thus, the spin Hall angle determined previously by the SP or SS was significantly underestimated, particular for those structure with a thin layer thickness.

Next we consider whether a similar correction is needed for the measurement of the spin Hall angle by the STT. When an external electric field E_0 applied in the plane of the layer, a non-uniform charge current $j_e(z) = \int dz \sigma_{||}(z, z') E_0 dz' \equiv \sigma_{||}(z) E_0$ generates a spin Hall electric field $E_s(z) = \theta_H \rho_N j_e(z)$ that drives a spin current perpendicular to the plane of the layers (CPP). The spin current then generates a spin accumulation $\mu_s(z)$ so that the effective spin electric field $E_s^{\rm eff}(z)$ is

$$E_s^{\rm eff}(z) = \theta_H \rho_N j_e(z) - \frac{d\mu_s}{dz}. \tag{4}$$

The linear response relation, $j_s(z) = \int \sigma_\perp(z, z') E_s^{\rm eff}(z') dz'$, where $\sigma_\perp(z, z')$ is the two point conductivity for the CPP, should be used to self-consistently solving for $E_s^{\rm eff}(z')$. In a previous study of the CPP spin transport, an approximate solution could be obtained when the spin diffusion length is much longer than the mean free path[25]: briefly, we invert the response function by writing $E_s^{\rm eff}(z) = \int \rho_s(z, z') j_s(z')$ and note that $j_s(z)$ varies with the length scale of spin diffusion length while the resistivity tensor $\rho_s(z, z')$ varies within the mean free path. We integrate over ρ_s , which yields a local resistivity ρ_N, i,e, the local Ohm's law $E_s^{\rm eff}(z) = \rho_N j_s(z)$ is valid[25], or

$$j_s(z) = \theta_H j_e(z) - \rho_N^{-1} \frac{d\mu_s}{dz} \tag{5}$$

By placing it to the rate equation of the spin current, $\boldsymbol{\nabla} \cdot \mathbf{j}_s = -\mu_s g_e/\tau_{sf}$ where τ_{sf} is the spin-flip time and g_e is the electron density of states, we have,

$$\frac{d^2\mu_s}{dz^2} - \frac{\mu_s}{\lambda_s^2} = \rho_N \theta_H \frac{dj_e(z)}{dz} \tag{6}$$

where λ_s is the diffusion length. Note that the above diffusion equation has a source term at the right side of the equation when the in-plane current density varies spatially. To solve Eqs. (5-6), we use the boundary condition at the outer boundary, $j_s(d_N) = 0$, and at the interface, $j_s(0) = -g_{mix}\mu_s$ where g_{mix} is the mixing conductance. We further use the fact that the source term varies with the mean free path while μ_s with λ_{sd}, and thus we replace $j(z)$ by its average and find

$$j_s(0) = \theta_H \frac{g_{mix}\left(1 - \operatorname{sech}\frac{d_N}{\lambda_s}\right)}{g_N \tanh\frac{d_N}{\lambda s} + g_{mix}} \frac{1}{d_N}\int_0^{d_N} j_e(z)dz \tag{7}$$

where we have introduced $g_N = 1/(\rho_N \lambda_s)$. The STT measures the current induced spin torque which is equivalent to the transverse component of spin current relative to the magnetization direction of the magnetic layer. Clearly, the spin Hall angle measurement based on the STT does not contain the factor $\rho_N \sigma_{||}(z)$. However, the determination of the current in the heavy metal $I_N = \int_0^{d_N} j_e(z)dz$ in Eq. (7) could be nontrivial. In the conventional treatment of the current distribution, the current density in the nonmagnetic layer is estimated via the resistance-in-parallel model for the two layers, i.e., taking $I_N = I_t \sigma_N t_N/(\sigma_N t_N + \sigma_F t_F)$ where I_t is the total applied current, σ_i and t_i $(i = N, F)$ are conductivities of the isolated layers and the thickness of the layer, respectively. We will show later that this rough approximation is usually smaller than the actual I_N for the coupled bilayers. Thus, for a given experimental spin torque, Eq. (7) would produce an overestimation of the spin Hall angle.

It is interesting to compare Eq. (2) and Eq. (7) with the giant magnetoresistance (GMR) of magnetic multilayers in the CIP and CPP geometries[26,27]. For CIP, the electric field is independent of position, and thus the spin and electric current densities are given by the two-point conductivity which has a length scale of the mean free path. If two magnetic layers are separated more than the mean free path by the nonmagnetic layer, the resistivity in one magnetic layer would be independent of the other magnetic layers and the magnetoresistance vanishes[28–30]. For the CPP case, the spin current densities are constant within the spin diffusion length, while the total electric field (the applied plus the induced ones) depends on

position. If one similarly introduces a two-point resistivity tensor, $\rho_\perp(z,z') = [\sigma_\perp(z,z')]^{-1}$, one finds a local Ohm's law remains valid, i.e., $E_s^{\rm eff}(z) = \rho(z) j_s$; this is the model of resistance in series and the current density will be determined by the resistance in series in all the layers. The CPP magnetoresistance does not decay exponentially with the mean free path, instead, the much longer spin diffusion length is the relevant length scale for the CPP GMR[25,31]. Equations (2) and (7) involve essentially the same mathematical features for the CIP and CPP spin transport.

B. Calculation of Nonlocal Conductivity

We now proceed to evaluate the position-dependence of the current density. For the SP or SS, we need to find $\rho_N \sigma_{||}(z)$, while for STT, we determine the average current density in the non-magnetic layer compared to the total applied current. We outline our model and calculation below. When there are no interface states, the simplest way to calculate $\sigma_{||}(z)$ is by using the semiclassical Boltzmann equation in which the position dependent distribution function is obtained via boundary conditions[32,33]. Another approach is to utilize the linear response theory or the Kubo formula to evaluate the two point conductivity, which can be expressed in terms of real space Green's functions[34–36]. The position-dependent conductivity, with varying impurity distribution, layer thickness and interface roughness, has been calculated across the magnetic multilayers. All of these approaches assume that the role of the interface is to scatter conduction electrons, i.e., the interface is treated as a boundary condition for the distribution function. We should extend the approach of Ref.[34–36] by explicitly including the cases when the differences in the electronic states for the interface and for the bulk are present.

A simple model Hamiltonian of the bilayer is chosen,

$$H = H_0 + H' \tag{8}$$

where $H_0 = H_L + H_R + H_{int}$ is the sum of the Hamiltonians for the left layer, the right layer, and the interface monolayer, H' describes the coupling between the interfacial monolayer and the left/right layers. More explicitly,

$$H_L = -t \sum_{\langle i,j\rangle \in L, \mathbf{k}_\parallel} \left(c^+_{i\mathbf{k}_\parallel} c_{j\mathbf{k}_\parallel} + h.c. \right) + \sum_{i\in L} c^+_{i\mathbf{k}_\parallel} \varepsilon^L_{\mathbf{k}_\parallel} c_{i\mathbf{k}_\parallel} \tag{9}$$

for the left layer and similarly for the right layer (replacing L by R in the above equation), where t is the hopping strength between the two nearest neighbors, $c^+_{i\mathbf{k}_\parallel} = \left(c^+_{i\mathbf{k}_\parallel\uparrow}, c^+_{i\mathbf{k}_\parallel\downarrow}\right)$ is conduction electron creation operator at site i, expressed in the spinor form. Note that we have written the Hamiltonian in the mixed space-momentum representation: the translation invariance in the plane of the layer allows us to use the in-plane momentum $\mathbf{k}_{||}$ as a quantum number while we retain the layered index i to represent the growth direction.

The Hamiltonian of the interface is

$$H_{int} = \sum_{\mathbf{k}_\parallel} c^+_{0\mathbf{k}_\parallel} \varepsilon_{0\mathbf{k}_{||}} c_{0\mathbf{k}_\parallel} \tag{10}$$

where the sub-index "0" indicates the interface layer, and $\varepsilon_{0\mathbf{k}_{||}}$ is the interface energy dispersion which could be spin-dependent.

The interaction between the interface and left/right layers is modeled by

$$H' = -t_L \sum_{\mathbf{k}_\parallel} c^+_{0\mathbf{k}_\parallel} c_{-1\mathbf{k}_\parallel} - t_R \sum_{\mathbf{k}_\parallel} c^+_{0\mathbf{k}_\parallel} c_{1\mathbf{k}_\parallel} + h.c. \tag{11}$$

where $t_{L/R}$ is the hopping parameter between the interface and the left/right layer. Note that the left (right) layer is indexed with a negative (positive) integer i representing the atomic position at $z = ia$; thus $i = -1$ and $i = 1$ are two atomic layers in contact with the interface layer $i = 0$.

The two-point conductivity for the layered structure can be obtained by the Kubo formula[34,36]

$$\sigma_{||}(i,j) = \frac{\hbar e^2}{\pi a^3} \sum_{\mathbf{k}_\parallel} v_{\mathbf{k}_\parallel}(i) A\left(i,j;E_F,\mathbf{k}_\parallel\right) v_{\mathbf{k}_\parallel}(j) A\left(j,i;E_F,\mathbf{k}_\parallel\right) \tag{12}$$

where i,j are atom sites along direction normal to interfaces, $A\left(i,j;E_F,\mathbf{k}_\parallel\right) = \frac{i}{2}\left[G_a\left(i,j;E_F,\mathbf{k}_\parallel\right) - \left[G_r\left(i,j;E_F,\mathbf{k}_\parallel\right)\right]\right.$ is the spectral density function, $G_{a/r}$ is the advanced/retarded Green's function, $v_{\mathbf{k}_\parallel} = \partial\varepsilon_{k_\parallel}/\hbar\partial\mathbf{k}_\parallel$ is the velocity operator of the local bands for left, interface or right layers. Note that Green's function and the velocity are spinors if the Hamiltonian is spin-dependent.

III. RESULTS AND DISCUSSION

We now apply the above two-point conductivity to a particular bilayer consisting of NiFe and Pt layers. We first assume there is no interface state and define a parameter p charac-

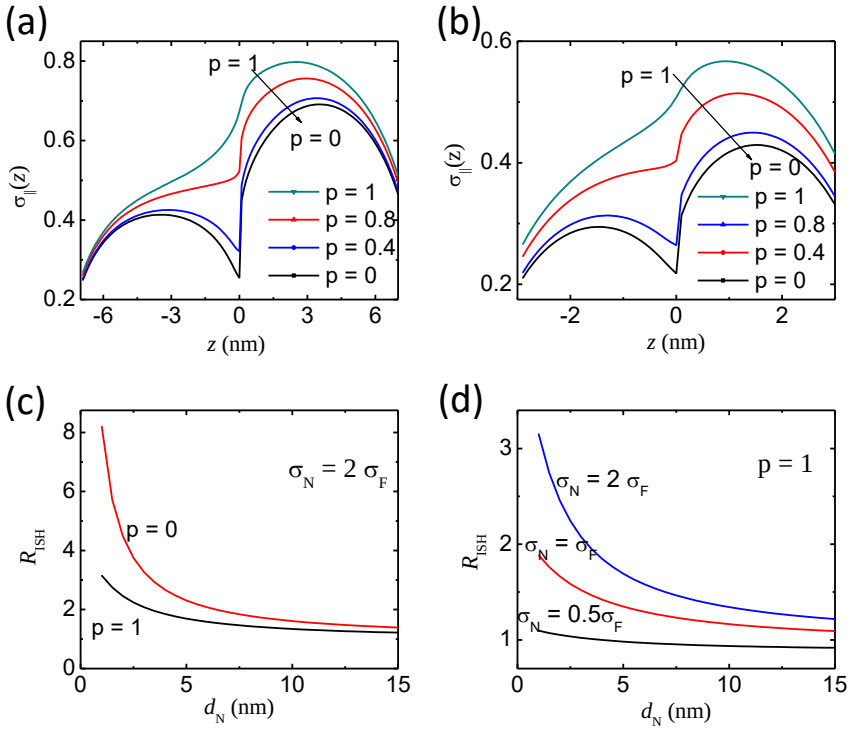

FIG. 2: (Color Online) (a) and (b): Spatial dependence of the electric conductivity across a FM ($z < 0$)/NM ($z > 0$) bilayer for different film thickness. The magnitude of the conductivity is normalized by the bulk value of the NM layer. c) and d): The enhancement factor $R_{\rm ISH}$ as a function of NM layer thickness. The electron diffusive scattering probability at the interface is parameterized by $1 - p$ where p is the probability of the electron passing through the interface without being scattered. The reflection of the electron at the interface is ignored and we assume the density of states of FM and NM layers are the same. The parameters in (a-c) are the mean free paths $\lambda_N = 10$ nm and $\lambda_F = 5$ nm, and the spin diffusion length $\lambda_s = 10$ nm. In (d), three different $\lambda_F = 20, 10, 5$ nm are shown.

terizing the degree of the smoothness of the interface ($p = 0$ for completely rough interface and $p = 1$ is completely smooth interface, and we takes $p = 0$ at the outer boundaries), as introduced by Fuchs[32]. The room-temperature resistivity values of NiFe and Pt are taken as $\rho_{\rm NiFe} = 40\ \mu\Omega cm$, and $\rho_{\rm Pt} = 25\ \mu\Omega cm$[16]. In Fig. 2 (a) and (b), we show the position-dependence of the reduced conductivity $\sigma_r \equiv \rho_N \sigma_{||}(z)$ for two different thickness. The σ_r is always smaller than 1 in the non-magnetic layer due to additional scattering from the interface. The reduction of σ_r is more profound for smaller thickness; this has been well known

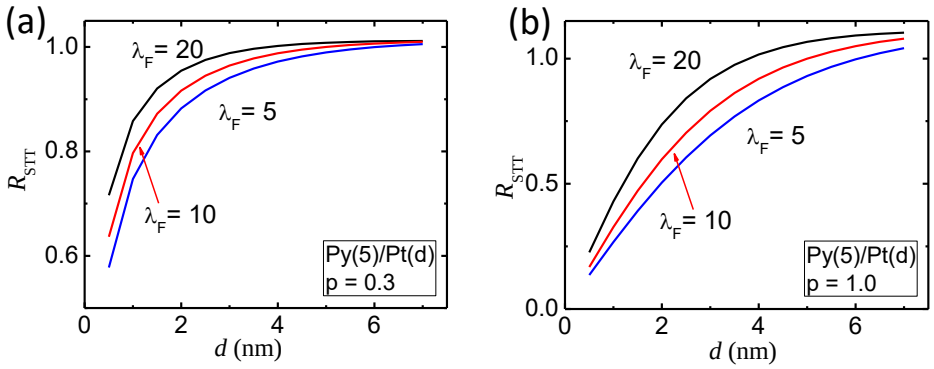

FIG. 3: (Color Online) (a) and (b):The calculated $R_{\rm STT}$ as a function of NM layer thickness. In above calculation, we set the mean free path of the NM layer to be 10 nm and that of FM layer is varied as 5, 10, 20 nm. The thickness of the FM layer is fixed to be 5 nm while that of NM layer changes from 0.5 to 7 nm.

that the enhancement contribution of the resistivity from the surface/interface scattering.

Using these numerical values, we can readily show the correction of the spin Hall angle to the previous measured $\theta_H^{\rm ISH}$, as plotted in Fig. 2(c). For example, for $d_N = 7$ nm and a rough interface $p = 0$, we find $R_{\rm ISH} = 2$, or the spin Hall angle was underestimated by a factor of two. The ferromagnetic conductivity can affect the enhancement factor as well. In Fig. 2(d), we show $R_{\rm ISH}$ as a function of NM layer thickness for three different FM conductivity with a smooth interface ($p = 1$). Clearly, the influence of the ferromagnetic layer is diminished when the interface is rough ($p = 0$).

Next, we evaluate the correction of the spin Hall angle in the STT experiment. Conventionally, the current in NM layer I_N is estimated from the parallel conductance of the two layers. For the interface with $p = 0$, this approximation is valid since the conductivity at one layer is independent of the the other and thus the STT experiment measures the correct spin Hall angle. For the case of $p \neq 0$, the adjacent FM layer enhances the conductivity of the NM layer which leads to a higher I_N compared to that of simple estimation when the NM layer thickness is small. We show in Fig. 3 the enhancement factor $R_{\rm STT} \equiv \theta_H/\theta_H^{\rm STT}$ due to the correction of the current distribution. Since most of the experimental analysis[8,9] was carried out with the Pt thickness less than 5nm, $R_{\rm STT}$ is significantly smaller, i.e., the spin Hall angle previously deduced from the STT experiment had been overestimated.

Recently, there is growing evidence that the spin-charge conversion also takes place at the

interface[6,37–44]. In the presence of large spin-orbit coupling known as the Rashba interaction, a spin helix state exists at the transition metal interface, but not in the bulk. In this case, the current density distribution at the interface could significantly differ from the bulk and thus the proper determination of the spin and charge currents in the layer and at the surface becomes a challenging issue, see Appendix. Aside from the complication of the current density distribution, other effects enter. In the SP, the interface leads to the spin memory loss[45–47], in the meanwhile, it creates an interface inverse Edelstein effect[48]. For the STT, there are complications on the relative contributions of the spin torque from the interface and bulk. In general, the quantitative determination of the interface versus bulk from the present experiments of SP and STT is difficult, we nevertheless propose that if the spin Hall and inverse spin Hall effects have independent contribution from the interface and from the bulk, a simple additive formula for the measured electric field by the spin pumping or spin Seebeck is,

$$E_m = G_t^{-1} j_s(0) \left[\rho_N \theta_H \int_0^{d_N} dz \sigma_{||}(z) \sinh \frac{d_N - z}{\lambda_s} + \lambda_{IEE} \right] \tag{13}$$

where λ_{IEE} characterizes the interface spin-to-charge conversion rate (in the unit of length); λ_{IEE} had been measured for α-Tin/Ag and Bi/Ag interfaces[49,50]. Similarly, for the STT experiment, one includes the interface contribution,

$$j_s(0) = \theta_H \frac{g_{mix} \left(1 - \mathrm{sech} \frac{d_N}{\lambda_s}\right)}{g_N \tanh \frac{d_N}{\lambda s} + g_{mix}} \frac{1}{d_N} \int_0^{d_N} j_e(z) dz + q_{EE} a_0 j_e^i \tag{14}$$

where j_e^i is the electrical current at the interface, a_0 is the interface lattice constant, and q_{EE} is the charge-to-spin conversion rate at the interface (in the unit of the inverse length) which has been measured for α-Tin/Ag interface[51] .

In summary, we have developed a quantitative model to address the determination of the spin Hall angle by different experimental methods. We find that by including the non-local conductivity, we are able to resolve a long standing controversy of inconsistent spin Hall angles derived from experiments of the spin pumping and the spin transfer torque. The authors thank Prof. Haifeng Ding from Nanjing University for sharing with us his experimental data prior to publication. This work was partially supported by National Science Foundation under Grant No. ECCS-1708180.

Appendix Conductivity contribution of interface states

In this appendix, we discuss the current density in thin films with interface states that take a variety of forms. In semiconductor heterostructure, the band mismatch of two layers could generate an interface band structure hosting a 2D-electron gas and the electron conduction is strictly limited at the interface region. In the presence of large spin-orbit coupling known as the Rashba interaction, a spin helix state exists at the transition metal interface, but not in the bulk. Let's first consider generic two-dimensional states formed at the interface and the coupling between the 2d states and nearest neighbor atoms is modeled by Eq. (11). The conductivity at the interface can be written as

$$\sigma(0) = \sigma(0,0) + \sum_j \sigma(0,j) \tag{A1}$$

which contains both the local and non-local contributions.

The Green's function at the isolated interface is,

$$g^{int}\left(n_0, n_0; E, \mathbf{k}_\parallel\right) = -\frac{1}{2t\cos ka} = \frac{1}{E - \varepsilon^{int}_{\mathbf{k}_\parallel} \pm i\Delta_{im}} \tag{A2}$$

where Δ_{im} is the impurity induced self energy. With finite interlayer hopping, one can show that the Green's function has a similar form,

$$G^0_{a/r}(0,0;E_F,\mathbf{k}_\parallel) = \frac{1}{E_F - \varepsilon_{0\mathbf{k}_\parallel} \pm i\left(\Delta_{im} + \Delta_T\right)} \tag{A3}$$

where

$$\Delta_T \equiv t_L^2 \mathrm{Im}[G^0(-1,-1;E_F,\mathbf{k}_\parallel)] + t_R^2 \mathrm{Im}[G^0(1,1;E_F,\mathbf{k}_\parallel)] \tag{A4}$$

is the self-energy introduced by hopping. So that when considering the interface conductivity, the hopping has two roles: on one hand it increases the self-energy at the interface and increases the non-local conductivity.

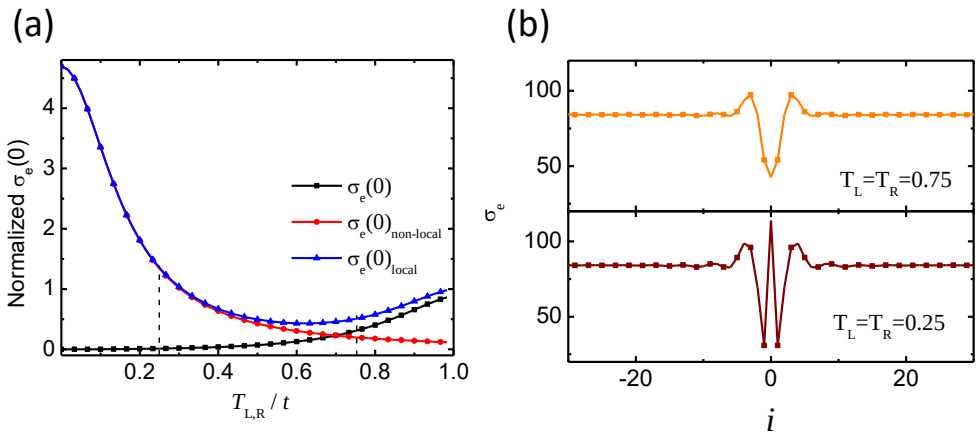

FIG. A1: (Color Online) (a). The local and nonlocal contributions to the interface conductance as a function of the coupling between 2d and 3d states. In our calculation, we took $k_F a = 1$. (b). The current distribution throughout the bilayer for fixed hopping parameters.

When the hopping parameters between 2d and 3d states are turned off, the interface and bulk current densities are independent. In terms of the Green's function, we have $G_{R/A}(0, i) = 0$. In Fig, A1(a), we show the interface conductance $\sigma(0)$ when $t_L = t_R$ turns on. The contribution from the $\sigma_L = \sigma(0, 0)$ decreases as the hopping increases, due to the enhanced relaxation from 2d states to 3d states, Eqs (A3, A4). On the contrary, the non-local contribution $\sigma_{NL}(0) = \sum_{j\neq 0} \sigma(0, j)$ begins to show up. Interestingly, the total interface conductance $\sigma(0) = \sigma_L(0) + \sigma_{NL}(0)$ has a local minimum at around $t_L = t_R \simeq 0.6t$. If we take a fixed value of $t_L = t_R$, the position dependent conductance are shown in Fig. A1(b). We notice that the current density shows a non-monotonic variation, which results from the opposite dependence of the local and nonlocal contribution on the interlayer hopping. For small interlayer hopping, the conductivity at the interface is dominated by the local contribution, increasing $t_{L/R}$ increases the self-energy in Eq. (A4) which in turn reduces the conductivity. For larger hopping, $t_{L/R} > 0.7t$, the self-energy is in Eq. (A4) is so large that the conductivity $\sigma(0)$ mainly comes from the non-local contribution. As $t_{L/R}$ keeps rising up, the Green's function $G(0, i)$ increases and so does the conductivity.

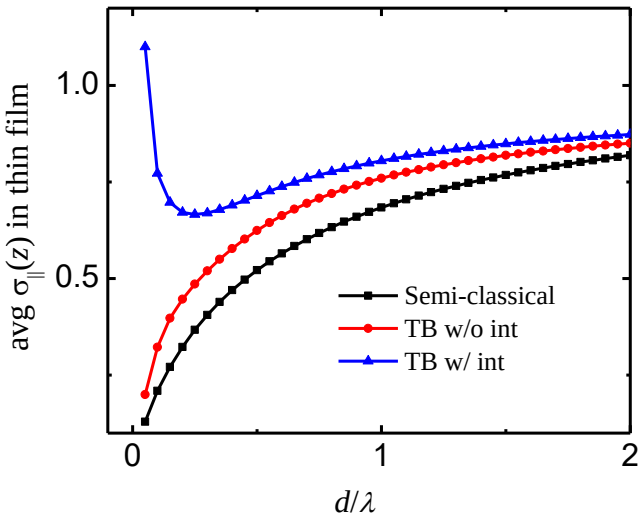

FIG. A2: (Color Online) The conductivity of a thin film with and without surface states as a function of layer thickness, λ is the electron mean free path in the bulk. When there is no surface states, the semiclassical continuous model (black square line) and our tight-binding approach (red circle line) are approximately same. In the presence of the surface state (c), the conductivity increases at the small thickness. The parameters used here: Rashba split is $0.2E_F$, mean free path 5 nm, the interfacial hopping $t_L/t = 0.4$.

For another example, we consider the thickness dependence of the conductivity when interface states are at present. We model the interface dispersion by,

$$\varepsilon_{0\mathbf{k}} = \varepsilon_0 + \frac{\hbar^2 k^2}{2m} + \hbar\alpha_F \left(\mathbf{k} \times \boldsymbol{\sigma}\right) \cdot \hat{z}, \tag{A5}$$

we find the current has a higher density at the interface than that in the bulk. The average conductivity for a thin film is shown in Fig. A2 for the plausible parameters.

[1] J. E. Hirsch, Phys. Rev. Lett. **83**, 1834 (1999).

[2] Jairo Sinova, Sergio O. Valenzuela, J. Wunderlich, C. H. Back, and T. Jungwirth, Rev. Mod. Phys. **87**, 1213 (2015).

[3] Y. K., Kato, R. C. Myers, A. C. Gossard, and D. D. Awschalom, Science **306**, 1910-1913 (2004).

[4] L. Liu, T. Moriyama, D. C. Ralph, and R. A. Buhrman, Phys. Rev. Lett. **106**, 036601 (2011).

[5] C.-F. Pai, L. Liu, Y. Li, H. W. Tseng, D. C. Ralph, and R. A. Buhrman, Appl. Phys. Lett. **101**, 122404 (2012).

[6] A. R. Mellnik, J. S. Lee, A. Richardella, J. L. Grab, P. J. Mintun, M. H. Fischer, A. Vaezi, A. Manchon, E.-A. Kim and N. Samarth, Nature **511**, 449 (2014).

[7] Luqiao Liu, Chi-Feng Pai, Y. Li, H. W. Tseng, D. C. Ralph, R. A. Buhrman, Science **336**, 555 (2012).

[8] W. Zhang, W. Han, X. Jiang, S.-H. Yang and S. S. P. Parkin, Nat. Phys. **11**, 496502 (2015).

[9] X. Zhou, M. Tang, X. L. Fan, X. P. Qiu, and S. M. Zhou, Phys. Rev. B **94**, 144427 (2016).

[10] M. Cecot, L. Karwacki, W. Skowronski, J. Kanak, J. Wrona, A. Zywczak, L. Yao, S. van Dijken, J. Barnas, T. Stobiecki, arXiv:1612.03020

[11] J. Kim, P. Sheng, S. Takahashi, S. Mitani, and M. Hayashi, Phys. Rev. Lett. **116**, 097201 (2016).

[12] K.-U. Demasius *et al.* Nat. Commun. **7**, 10644 (2016).

[13] Z. Feng, J. Hu, L. Sun, B. You, D. Wu, J. Du, W. Zhang, A. Hu, Y. Yang, D. M. Tang, B. S. Zhang, and H. F. Ding, Phys. Rev. B **85**, 214423 (2012).

[14] H. Nakayama, K. Ando, K. Harii, T. Yoshino, R. Takahashi, Y. Kajiwara, K. Uchida, Y. Fujikawa, and E. Saitoh, Phys. Rev. B **85**, 144408 (2012).

[15] O. Mosendz, V. Vlaminck, J. E. Pearson, F. Y. Fradin, G. E. W. Bauer, S. D. Bader, and A. Hoffmann, Phys. Rev. B **82**, 214403 (2010).

[16] V. Vlaminck, J. E. Pearson, S. D. Bader, and A. Hoffmann, Phys. Rev. B **88**, 064414 (2013).

[17] C. Hahn, G. de Loubens, O. Klein, M. Viret, V. V. Naletov, and J. Ben Youssef, Phys. Rev. B **87**, 174417 (2013).

[18] A. Azevedo, L. H. Vilela-Leão, R. L. Rodrìguez-Suárez, A. F. Lacerda Santos, and S. M. Rezende, Phys. Rev. B **83**, 144402 (2011).

[19] H. L. Wang, C. H. Du, Y. Pu, R. Adur, P. C. Hammel, and F. Y. Yang, Phys. Rev. Lett. **112**, 197201 (2014).

[20] F. Freimuth, S. Blügel, and Y. Mokrousov, Phys. Rev. B **92**, 064415 (2015).

[21] L. Wang, R. J. H. Wesselink, Y. Liu, Z. Yuan, K. Xia, and P. J. Kelly, Phys. Rev. Lett. **116**, 196602 (2016).

[22] Y. Wang, P. Deorani, X. Qiu, J. H. Kwon, and H. Yang, Appl. Phys. Lett. **105**, 152412 (2014).

[23] Minh-Hai Nguyen, D. C. Ralph, and R. A. Buhrman, Phys. Rev. Lett. **116**, 126601 (2016).

[24] O. Mosendz, J. E. Pearson, F. Y. Fradin, G. E. W. Bauer, S. D. Bader, and A. Hoffmann, Phys. Rev. Lett. **104**, 046601 (2010).

[25] H. E. Camblong, S. Zhang, and P. M. Levy, Phys. Rev. B **47**, 4735 (1993).

[26] M. N. Baibich, J. M. Broto, A. Fert, F. Nguyen Van Dau, F. Petroff, P. Etienne, G. Creuzet, A. Friederich, and J. Chazelas, Phys. Rev. Lett. **61**, 2472 (1988).

[27] G. Binasch, P. Grunberg, F. Saurenbach, and W. Zinn, Phys. Rev. B **39**, 4828 (1989).

[28] A. Barthelemy, A. Fert, Phys. Rev. B, **43**, 13124 (1991).

[29] A. Vedyayev, B. Dieny, N. Ryzhanova, Europhys. Lett., **19** 329 (1992).

[30] J. Barnas, Y. Bruynseraede, Phys. Rev. B, **53**, 5449 (1996).

[31] T. Valet, and A. Fert, Phys. Rev. B, **48**, 7099 (1993).

[32] K. Fuchs, Proc. Camb. Phil. Soc. **34**, 100 (1938).

[33] E. H. Sondheimer, A. H. Wilson, Proc. Royal Soc. **190** 435 (1947).

[34] A. Vedyayev, B. Dieny and N. Ryzhanova, Europhys. Lett. **19**, 329 (1992).

[35] Y. Asano, A. Oguri, and S. Maekawa, Phys. Rev. B **48**, 6192 (1993).

[36] H. E. Camblong, P. M. Levy and S. Zhang, Phys. Rev. B **51**, 16052 (1995).

[37] A. Manchon and S. Zhang, Phys. Rev. B, **78**, 212405 (2008).

[38] M. Jamali, K. Narayanapillai, X. Qiu, L. M. Loong, A. Manchon, and H. Yang, Phys. Rev. Lett. **111**, 246602 (2013).

[39] Miron, I. M. et al. Nature Mater. **9**, 230-234 (2010).

[40] Y. Fan *et al.*, Nat. Mater. **13**, 699 (2014).

[41] X. Fan, H. Celik, J. Wu, C. Ni, K.-J. Lee, V. O. Lorenz and J. Q. Xiao, Nat. Commun. **5**, 3042 (2014).

[42] S. Zhang, and A. Fert, Phys. Rev. B, **94**, 184423 (2016).

[43] J.-C. Rojas-Sánchez, S. Oyarzún, Y. Fu, A. Marty, C. Vergnaud, S. Gambarelli, L. Vila, M. Jamet, Y. Ohtsubo, A. Taleb-Ibrahimi, P. Le Fèvre, F. Bertran, N. Reyren, J.-M. George, and A. Fert, Phys. Rev. Lett. **116** , 096602 (2016).

[44] F. Mahfouzi, N. Nagaosa, and B. K. Nikolić, Phys. Rev. B **90**, 115432 (2014).

[45] Mazin A. Khasawneh, Carolin Klose, W. P. Pratt, Jr., and Norman O. Birge, Phys. Rev. B **84**, 014425 (2011).

[46] J.-C. Rojas-Sánchez, N. Reyren, P. Laczkowski, W. Savero, J.-P. Attané, C. Deranlot, M. Jamet,

J.-M. George, L. Vila, and H. Jaffrès, Phys. Rev. Lett. **112**, 106602 (2014).

[47] K. Chen, and S. Zhang, Phys. Rev. Lett. **114**, 126602 (2015).

[48] Ka Shen, G. Vignale, and R. Raimondi, Phys. Rev. Lett. **112**, 096601 (2014).

[49] J.-C. Rojas-Sánchez, L. Vila, G. Desfonds, S. Gambarelli, J. P. Attané, J. M. De Teresa, C. Magén, and A. Fert, Nat. Commun. **4**, 2944 (2013).

[50] J.-C. Rojas-Sánchez, S. Oyarzún, Y. Fu, A. Marty, C. Vergnaud, S. Gambarelli, L. Vila, M. Jamet, Y. Ohtsubo, A. Taleb-Ibrahimi, P. Le Fèvre, F. Bertran, N. Reyren, J.-M. George, and A. Fert, Phys. Rev. Lett. **116**, 096602

[51] K. Kondou, R. Yoshimi, A. Tsukazaki, Y. Fukuma, J. Matsuno, K. S. Takahashi, M. Kawasaki, Y. Tokura, and Y. Otani, Nat. Phys. **12**, 1027 (2016).